ELSEVIER

Polymer 42 (2001) 5771–5779

polymer

www.elsevier.nl/locate/polymer

Molecular shape of poly(2-ethyl-2-oxazoline) chains in THF

J.H. Sung[a], D.C. Lee[b,*]

[a]*Kyung-in Regional Korea Food and Drug Administration, 7-241 Sinheung-dong 3, Chung-gu, Inchun, South Korea*
[b]*Department of Polymer Science and Electrical Engineering, Inha University, Inchon 402-751, South Korea*

Received 15 August 2000; received in revised form 26 October 2000; accepted 20 November 2000

Abstract

The molecular shape of well-defined poly(2-ethyl-2-oxazoline) (PEOz) chains in tetrahydrofuran (THF) at room temperature has been studied by a combination of static and dynamic light scattering and viscometry in the framework of the hard-sphere model. Data of the z-average radius of gyration as well as equivalent sphere radii such as the hydrodynamic radius (R_H), the viscometric radius (R_V), and the thermodynamic radius (R_T) give some evidences of sphere-like structure. The unperturbed molecular dimension ($(\langle R_G^2\rangle_0/M_w)_\infty^{1/2} = 624 \times 10^{-4}$ nm) determined by an indirect method and the persistence length $q = 0.70$ nm determined by the Bushin–Bohdanecky method appear to be quite small compared to those of common flexible polymers. In particular, the R value (24.0), defined by $\langle R_G^2\rangle^{1/2}/q$, being of a considerably higher order than unity allows an estimation that the chain possibly has a type of "random Gaussian globule". Based upon the experimental results so far obtained, it can be concluded that the chains of PEOz in THF at 25°C assume basically a shape that is very similar to that of a sphere in the least draining limit. Both the branch-like structure of the PEOz molecule and the intramolecular polar interaction between the nitrogen of the main chain and the carbonyl carbon in the side group are considered to be responsible for the chain contraction. © 2001 Published by Elsevier Science Ltd.

Keywords: Poly(2-ethyl-2-oxazoline); Molecular shape; Sphere-like structure

1. Introduction

Since the first work on the polymerization of 2-aryl- and 2-alkyl-2-oxazolines in the 1960s, many investigations on these polymers have concentrated exclusively on the evaluation of polymerization mechanisms [1–7], which has led to the conclusion that two types of propagation route occur based on the active species [8–10]. However, little is known yet about their molecular characteristics and physical properties.

Recently, poly(2-ethyl-2-oxazoline) (PEOz) has received increasing attention in both the industrial and academic fields with the successful synthesis of soluble high molar mass products. Undoubtedly, this interest stems from PEOz's unusual properties and its potential applications as a new functional material. PEOz is an amorphous, non-ionic, and tertiary amide polymer exhibiting good solubility both in common organic solvents and in water. The material also exhibits excellent thermal stability, facile melt fabrication, miscibility with other various common thermoplastics, and non-toxicity [11–13]. Therefore, a major amount of research is currently being carried out in polymer blending [13] and block copolymer micelle formation for the drug delivery system [12].

Basically, the physical properties exhibited by a branched polymer can be understood in terms of inherent skeletal flexibility, with specific physical or chemical characteristics imposed by the side groups. The most striking effect exerted by the side groups is the conformational change of the backbone chain which, in turn, leads to the variation of the physical properties of the polymer. In particular, the phenomenon of chain collapse owing to the net attraction among parts of a single polymer molecule is of interest not only because of biological applications such as protein folding but also because of its fundamental importance as related to polymer microstructure and fractionation. Thus, from the theoretical and experimental point of view, the molecular characterization and the evaluation of the conformational characteristics are considered to be essential to understand the structure–property relationship better and to provide a better basis for the perfect molecular design to produce new functional materials. However, theoretical analyses and experimental data on the conformation of PEOz in common organic solvents are yet very few.

* Corresponding author.
E-mail addresses: polysung@hanmail.net (J.H. Sung), soldclee@dragon.inha.ac.kr (D.C. Lee).

0032-3861/01/$ - see front matter © 2001 Published by Elsevier Science Ltd.
PII: S0032-3861(00)00861-2

The purpose of the present study is to search for the molecular shape and conformational behavior of PEOz chains in tetrahydrofuran (THF) at 25°C. A variety of dilute solution techniques have been used to find the molecular shape and conformational parameters. Particular attention is given to the determination of the radius of gyration and various equivalent radii, and their ratios. The results obtained are interpreted in terms of the existing theories for the chain conformation and compared with theoretical predictions to offer a quantitative description of the molecular shape and dimensions for the given chain [14–19].

2. Experimental

2.1. Materials

PEOz was obtained from Aldrich Chemical Co. The THF was spectrograde supplied by Tedia Co. and used without further purification.

2.2. Solubility tests

The solubility tests were made by placing 0.1 g of polymer in 5 ml of the desired solvent and stirring for several hours or until all the polymer had gone into solution at 25°C. The solvents used were 25 kinds of organic compound, their solubility parameter ranging from 14.9 to 29.7 $MPa^{1/2}$. The results were compared with values estimated from the Hoftyzer–Van Krevelen and Hoy methods [20], respectively.

2.3. Fractionation

The fractionation was carried out by the column elution technique. The polymer-coated glass beads ($d = 0.5$ mm) were packed in a column and successive elution was carried out with a mixed solvent of increasing solvent power. The composition gradient was varied with time from 100% of non-solvent to 100% of good solvent. The dissolved polymer molecules were transferred to the top of the column, being eluted by the mixed solvent passing through the column upward at constant temperature. A fixed amount of the eluted fraction was collected and the polymer was recovered by solvent evaporation. The solvent–non-solvent system used was THF and *n*-Hexane. The temperature of the column was kept at 25°C. Seventeen fractions were used for the measurements.

2.4. Size exclusion chromatography

The GPC measurements for the determination of the polydispersity indices of those fractionated samples were carried out using Waters Model 201 equipped with a U6K injector, an M 6000A solvent delivery system, an M 730 data module, and four linear columns packed with μ-styragel. The flow rate of the carrier liquid (THF) was 0.1 ml/min and standard polystyrene was used for the calibration.

2.5. Viscometric measurement

An Ubbelohde suspended level type of viscometer was employed. A simultaneous extrapolation to infinite dilution of the plot η_{sp}/c and $\ln \eta_{rel}/c$ versus concentration, as usual, yielded the values of intrinsic viscosity ($[\eta]$) and Huggins constant (k_H).

2.6. Static light scattering

Scattered light intensities from PEOz in THF at 25°C were measured on a Brookhaven BI-200SM goniometer in an angular range from 20 to 155°. Incident light of 632.8 nm wavelength from the 35-mW He–Ne laser light source was used. Solutions, ranging in concentration from 0.7 to 15 mg/ml, were introduced into the cell with a syringe equipped with a 0.2-μm Millipore microfilter. The intensity data obtained were analyzed by a Zimm plot [21] to evaluate the mass-average molar mass (M_w), second virial coefficient (A_2), and z-average radius of gyration ($\langle R_G^2 \rangle^{1/2}$).

The specific refractive index increment for PEOz in THF at 25°C was 0.0738 ml/g. The Optilab DSP interferometric refractometer with wavelength 632.8 nm was employed.

2.7. Dynamic light scattering

The photoelectron count time correlation function [22] has the form:

$$G^{(2)}(t) = A(1 + b|g^{(1)}(t)|^2) \tag{1}$$

where $g^{(1)}(t)$ is the normalized electron field correlation function with t being the delay time, A the base line, and b a spatial coherence factor. For a polydisperse polymer solution,

$$|g^{(1)}(t)| = \int_0^\infty G(\Gamma) \exp(-\Gamma t)\, d\Gamma \tag{2}$$

where $G(\Gamma)$ is the normalized characteristic line-width distribution function with Γ as the z-average characteristic line-width. The photoelectron count time correlation function was measured by employing a Brookhaven BI-9000AT autocorrelator. Measurements were carried out for four to six dilute concentrations at nine angles for all the PEOz fractions. In most cases, values are accepted as the correlation function when the measured baseline agrees with the computed baseline within the error range of 0.1%. The effective hydrodynamic radius R_H of the polymer chain was calculated from the z-average translational diffusion constant D_0 by means of the well-known Stoke–Einstein equation [22]:

$$D_0 = (\langle \Gamma \rangle / q^2)_{c=0,\theta=0} = \frac{k_B T}{6\pi \eta_0 R_H} \tag{3}$$

where k_B is the Boltzmann constant and T is the absolute temperature.

3. Results and discussion

3.1. Dissolution behavior of PEOz in organic solvents

As is well known, the total solubility parameter δ_t of a polymer can be given by $\delta_t^2 = (\delta_d)^2 + (\delta_p)^2 + (\delta_h)^2$. For the practical determination of δ_t for PEOz, Bagley's two-dimensional method [23] was used, since it was based on a reasonable assumption that the effects of δ_d and δ_p were in close similarity while δ_h was quite different. Accordingly, they introduced the parameter δ_v defined by $\delta_v = \sqrt{(\delta_d)^2 + (\delta_p)^2}$. This leads to a diagram in which δ_h and δ_v are plotted on the axes. The solubility region then can be delimited by a circle with a radius of about five δ-units. Such a diagram is shown in Fig. 1 for 25 kinds of organic solvent at 25°C. By borrowing the values of Hansen's solubility parameter components for various solvents [20], the δ_t of PEOz can be estimated as 20.1 $MPa^{1/2}$, which is very close to the 19.4 $MPa^{1/2}$ of THF. Furthermore, a trend is immediately obvious from the diagram, i.e. that the solubility of PEOz depends strongly upon the parameter component δ_h rather than δ_v. This is the reason why the polymer can be dissolved easily in water and many other alcohols whose δ_h values are approximately above 10.2 $MPa^{1/2}$.

3.2. Static light scattering

Fig. 2 shows those plots of concentration dependence of scattered light intensities at zero angle $(Kc/R_\theta)_{\theta=0}$ for all the PEOz fractions. The values of M_w and A_2 are summarized in Table 1, together with the values of M_w/M_n determined by size exclusion chromatography. As evidenced from Fig. 2, the lines drawn show good linearity even in the region of

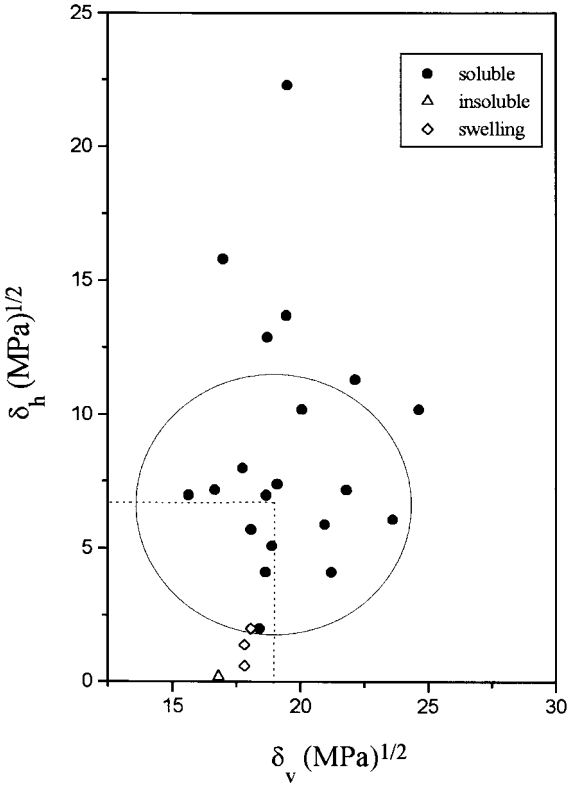

Fig. 1. Solubility behavior of PEOz in various solvents in the δ_h versus δ_v plot ($\delta_v = (\delta_p^2 + \delta_d^2)^{1/2}$).

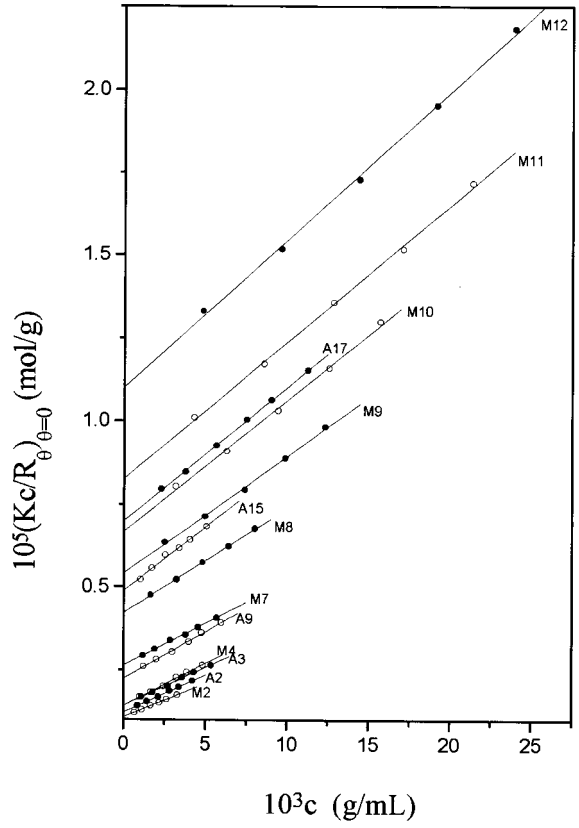

Fig. 2. Concentration dependence of scattered light intensities at zero angle for indicated PEOz fractions in THF at 25°C.

Table 1
Molecular characteristics of PEOz in THF at 25°C

Fraction code	$M_w \times 10^{-5}$ (g/mol)	$A_2 \times 10^4$ (cm^3 mol/g^2)	$[\eta]$ (dl/g)	k_H	M_w/M_n
M2	9.14	1.020	0.526	0.65	1.4
A2	7.97	1.123	0.488	0.49	1.4
M4	7.80	1.128	0.429	0.61	1.2
A3	6.80	1.127	0.443	0.68	1.4
A6	5.77	1.310	0.439	0.77	1.2
A9	4.36	1.420	0.393	0.58	1.2
M6	4.07	1.515	0.322	0.46	1.2
M7	3.75	1.260	0.300	0.63	1.2
A13	2.92	1.925	0.365	0.81	1.3
M8	2.36	1.574	0.283	0.74	1.1
A15	2.04	1.940	0.305	0.55	1.2
M9	1.84	1.769	0.264	0.61	1.1
M10	1.49	1.980	0.241	0.48	1.1
A17	1.41	2.010	0.247	0.49	1.2
M11	1.21	2.064	0.206	0.52	1.2
M12	0.91	2.230	0.177	0.62	1.2
A19	0.68	2.110	0.167	0.96	1.2

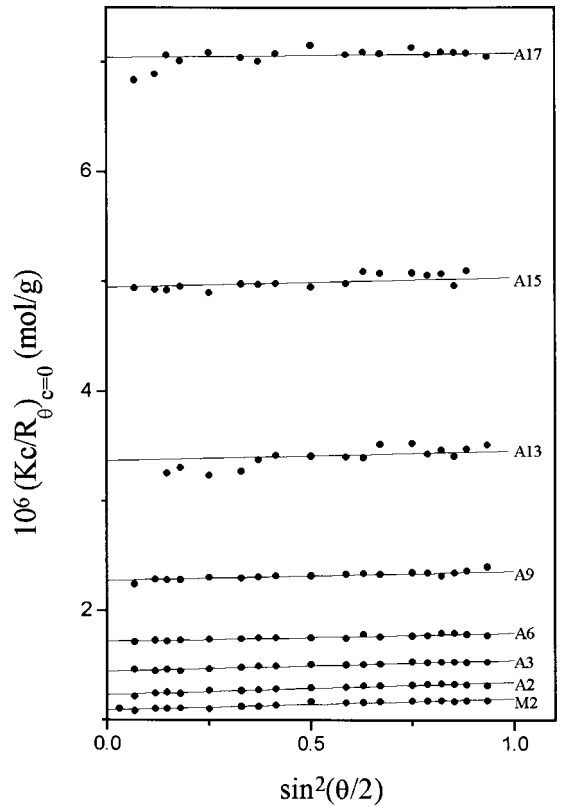

Fig. 3. Angular dependence of scattered light intensities at infinite dilution for indicated PEOz fraction in THF at 25°C.

low concentration. The M_ws found are in the range from 0.68×10^5 to 9.14×10^5 g/mol, and this span of molar mass is considered to be enough to provide accurate information for the molecular shape. The polydispersity indices of high molar mass fractions, however, appear as slightly large.

In Fig. 3, the angular dependence of scattered light intensities at infinite dilution $(Kc/R_\theta)_{c=0}$ are illustrated for all the fractions. The z-average root mean square radii of gyration $\langle R_G^2 \rangle^{1/2}$ are evaluated from the slopes of the corresponding straight lines, and their values are listed in Table 2 along with various other radii of spheres and their ratios. As is clear from Fig. 3, the low molar mass fractions (A13, A15, and A17) exhibit poor linearity and small slopes, and hence their $\langle R_G^2 \rangle^{1/2}$ values are excluded.

It is worth noting that the highest molar mass fraction (M2) reveals $\langle R_G^2 \rangle^{1/2} = 19.2$ nm, which is found to be smaller than 27.0 nm for PS in cyclohexane at 34°C, and 21.0 nm for PMMA in *n*-butyl chloride at 35.4°C, when compared on the same molar mass basis (9.14×10^5 g/mol) [24]. This low value suggests that a chain contraction arises from either the branch-like structure of the PEOz molecule or the intramolecular specific interaction.

The plot of $\langle R_G^2 \rangle^{1/2}$ dependence on molar mass, illustrated in Fig. 4, yielded the following power law:

$$\langle R_G^2 \rangle^{1/2} = 1.064 \times 10^{-2} M_w^{0.55} \text{ (nm)} \quad (4)$$

The exponent of 0.55 comes out smaller than the 0.60 in good solvent predicted from the mean field theory [25] for a flexible chain. Besides, this exponent reinforces that THF at 25°C is a thermodynamically moderate solvent for PEOz, since theory and experiment support 0.5 at the θ-state and ca. 0.588 [26,27] in the good solvent limit.

3.3. Second virial coefficient (A_2)

As Flory and Krigbaum [28] first proposed, the experimental data of A_2 reported for linear polymers in good and marginal solvents indicate, almost without exception, that A_2 is a decreasing function of molar mass. A_2 values found are summarized in Table 1. The plot of A_2 against M_w (Fig. 5) yielded the following relation:

$$A_2 = 6.737 \times 10^{-3} M_w^{-0.30} \text{ (cm}^3 \text{ mol/g}^2\text{)} \quad (5)$$

The exponent -0.30 exceeds the range of -0.20 to -0.22, which is the asymptotic value observed for very high M_w ($>10^7$) polymers regardless of the kind of solvent [29]. Although the exponent in poor solvent has not been explored much, the exponent -0.30, often observed for a typical linear flexible chain, is believed to be a consequence

Table 2
Size radii and their ratios of PEOz in THF at 25°C

Fraction code	$\langle R_G^2 \rangle^{1/2}$ (nm)	R_H (nm)	R_T (nm)	R_V (nm)	$\langle R_G^2 \rangle^{1/2}/R_H$	$\langle R_G^2 \rangle^{1/2}/R_T$	R_V/R_H	$\langle R_G^2 \rangle^{1/2}/R_V$
M2	19.2	15.9	20.4	19.7	1.21	0.94	1.24	0.98
A2	18.8	15.6	19.2	18.3	1.21	0.98	1.18	1.03
A3	16.4	14.7	17.3	16.8	1.12	0.95	1.15	0.97
A6	15.2	13.0	16.3	15.9	1.17	0.93	1.22	0.96
A9	14.4	11.0	13.9	14.0	1.32	1.04	1.27	1.03
A13		9.8	11.8	11.9			1.21	
M8		7.9	9.5	10.2			1.29	
A15		8.3	9.3	10.0			1.20	
M9		7.4	8.4	9.2			1.24	
A17		6.1	7.3	8.2			1.34	
A19			4.6	5.6				

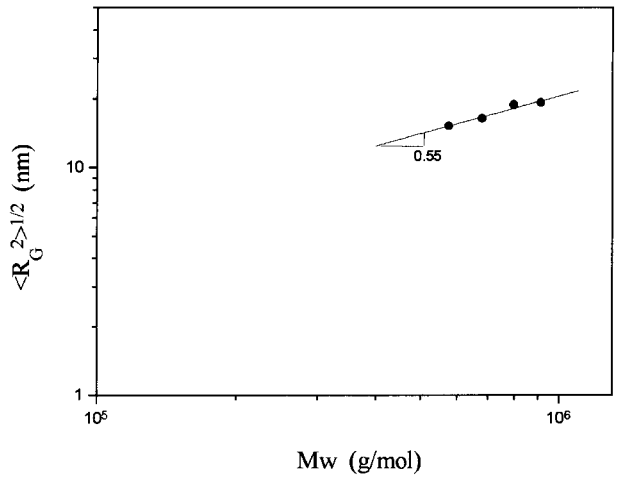

Fig. 4. Double-logarithmic plots of $\langle R_G^2 \rangle^{1/2}$ versus M_w for PEOz in THF at 25°C.

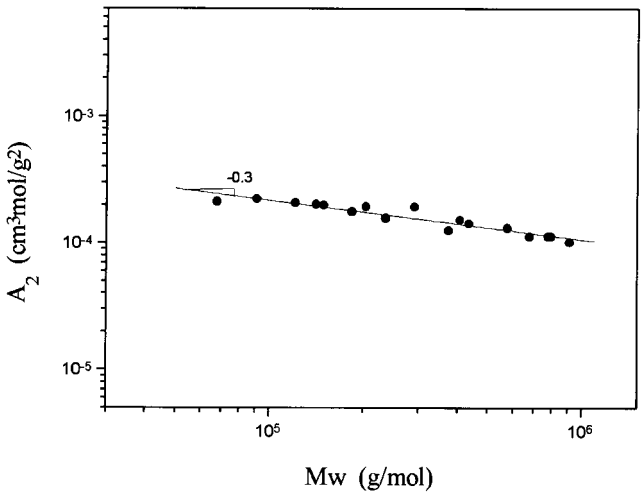

Fig. 5. Double-logarithmic plots of A_2 versus M_w for PEOz in THF at 25°C.

of a chain structure of PEOz molecules in THF somewhat different from the common linear flexible open chain.

A comparison of the present A_2 data of PEOz with those of Chen et al. [30], that is, $7.5–10.8 \times 10^{-4}$ in water, $19.5–22.6 \times 10^{-4}$ in ethanol, and $9.8–30.9 \times 10^{-4}$ cm^3 mol/g^2 in isopropanol, indicates that the A_2 value depends significantly on the solvent quality. As evidenced from the above comparison, the present A_2 values marked a substantially lower order of magnitude. One of the reasons for this behavior is the long-range intramolecular polar interaction, in a system of dilute solutions, between nitrogen in the main chain and carbonyl carbon in the side group. Concurrently, there may be a contribution of THF to the formation of intramolecular interaction.

Experimental data for dilute polymer solution properties are frequently presented in terms of equivalent spheres and their dimensionless ratios to discuss the molecular shape or chain conformation of a flexible polymer chain. The values of hard-sphere virial radius (or thermodynamic radius) R_T, estimated from the following equation [14,17]

$$R_T = \left[\frac{3M_w^2 A_2}{16\pi N_A} \right]^{1/3} \text{(nm)} \quad (6)$$

are tabulated in Table 2. They are found to be comparable with $\langle R_G^2 \rangle^{1/2}$s, on the same molar mass level. Theoretically, R_T corresponds to the radius of a hard sphere with the same excluded volume as the polymer coil and can be regarded as the radius of the sphere. Thus, R_T can be written as [14]:

$$R_T = (5/3)^{1/2} R_G \quad (7)$$

At the higher molar mass range ($>4.36 \times 10^5$), however, the R_T average of this study appears as 20% smaller than the theoretical $\langle R_G^2 \rangle^{1/2}$ value estimated by Eq. (7). This situation also suggests that the PEOz chain has a structure different from that of a typical random coil.

The power law established for the R_T is as follows:

$$R_T = 9.073 \times 10^{-3} M_w^{0.56} \text{ (nm)} \quad (8)$$

The value of the exponent that is somewhat lower than 0.6, which can be predicted from a typical flexible chain in a good solvent, seems to be due to the chain contraction. Moreover, the strong molar mass dependence of R_T, as is illustrated in Fig. 6, is attributed to the vanishing excluded-volume effect as the molar mass decreases.

3.4. Dynamic light scattering

Fig. 7 illustrates the concentration dependence of the apparent translational diffusion coefficient D [$= (\langle \Gamma \rangle / q^2)_{\theta=0}$] as a function of polymer concentration. D_0 from the intercept, and hence the hydrodynamic radius R_H can be calculated from the Stokes–Einstein relation. These are summarized in Table 2. The R_Hs found are smaller than those of PS in 2-butanone in which the chains are known to have a non-spherical shape [18]. Additionally, for a given molar mass, the R_H values in

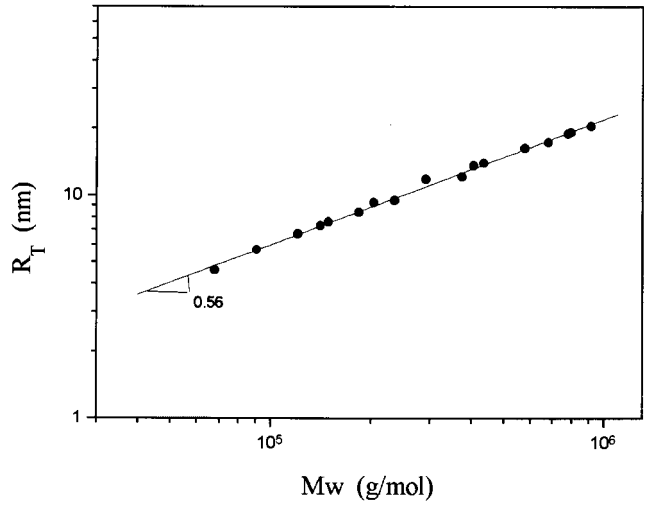

Fig. 6. Double-logarithmic plots of R_T versus M_w for PEOz in THF at 25°C.

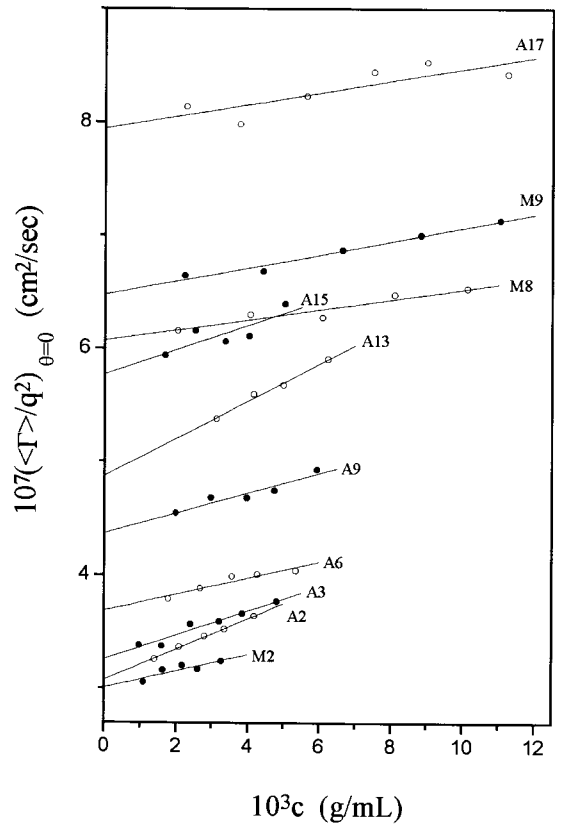

Fig. 7. Concentration dependence of $(\langle\Gamma\rangle/q^2)_{\theta=0}$ for indicated PEOz fractions in THF at 25°C.

Table 2 are found to be comparable to those of poly(ethyleneimine) fractions in 1 M NaCl aqueous solvent, in which the chains are known to adopt a compact and randomly branched structure [31]. This brief comparison also gives evidence that the chains of PEOz have a sphere-like structure.

The linear regression of the R_H data as a function of molar mass yielded the following power law:

$$R_H = 8.268 \times 10^{-3} M_w^{0.51} \text{ (nm)} \quad (9)$$

The exponent 0.51 is in the well outside the region where a polymer in thermodynamically good solvents can typically be revealed, and agrees with the value of 0.537 [= (0.55 × 2 + 0.51)/3], calculated using a rough approximation proposed by Weill and Cloizeaux [32]. If the hydrodynamic volume can be taken as the average conformational size of a dissolved flexible polymer, the decreasing trend of the hydrodynamic volume of PEOz with increasing molar mass clearly suggests the potential of the "random Gaussian globule" [33].

3.5. Viscosity

The values of intrinsic viscosity ($[\eta]$) and the Huggins constant (k_H) found are summarized in Table 1. Obviously, all the $[\eta]$ values estimated appear as somewhat lower than

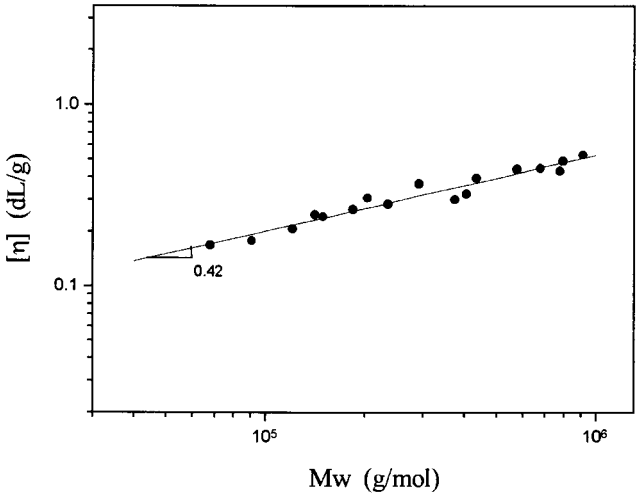

Fig. 8. Double-logarithmic plots of $[\eta]$ versus M_w for PEOz in THF at 25°C.

those revealed by the usual flexible linear polymers, on the same molar mass basis. This seems likely to be due to the smaller spatial extension of the branch-like structure of the PEOz chain, and is qualitatively consistent with the large values of the k_Hs, though their variation trend is not discernible [34].

The molar mass dependence of $[\eta]$ illustrated in Fig. 8 yields the following power law, strictly valid for the molar mass range indicated:

$$[\eta] = 1.601 \times 10^{-3} M_w^{0.42} \text{ (dl/g)} \quad (10)$$

$$(0.68 \times 10^5 \leq M_w \leq 9.14 \times 10^5), \text{ (g/mol)}$$

Numerous experiments confirm the exponent 0.5 for the unperturbed coils, while the renormalization group theory predicts 0.764 for the perturbed coils. In practice, however, small values (<0.764) are often found for perturbed coils in cases where some moderately good solvents or conformations of branched polymers are concerned. [31,35]. The low value of 0.42 for the exponent may be a consequence of the sphere-like structure formed by the smaller spatial extension and the higher segment density within the volume pervaded by a branched molecule. From the point of view of dimensional contraction, it has been found [36] that the uniformity in subchain length causes a greater contraction of the molecular dimensions so that a specific intramolecular interaction, a polar interaction between nitrogen in the main chain and carbonyl carbon in the side group, in a regular type of comb-like molecule like the PEOz molecule, is facile. Furthermore, the environment provided is a dilute solution system in which the overwhelming fractions of the chain can undergo intramolecular interaction. Similar behaviors are also reported for the aromatic polymers containing 2,4-quinoline units [37] and branched polyethyleneimine [31].

Table 3
Comparison of size ratios between model polymers and PEOz

Model	$\langle R_G^2\rangle^{1/2}/R_H$	$\langle R_G^2\rangle^{1/2}/R_T$	$\langle R_G^2\rangle^{1/2}/R_V$	R_V/R_H	Reference
Hard sphere	0.78	0.78	0.78	1	[54]
Gaussian coil	1.24		1.22	1.02	[55]
Non-draining-self-avoiding random work	1.56	1.52	1.37	1.14	[47,55]
Non-draining-Gaussian chain	1.24	1.41	1.24	1.02–1.04	[44]
Four-arm star PS in toluene	1.1	1.12	1.1	1.01	[46]
PEOz[a]	1.21	0.97	0.996	1.22	This work

[a] Values of high molar masses ($M_w > 4.36\times10^5$) are averaged.

The $[\eta]$ values listed in Table 1 yield the sphere viscometric radius R_V [17], and hence the following power law can be established:

$$R_V = 2.921\times10^{-2}M_w^{0.47}\ (\text{nm}) \quad (11)$$

The exponent 0.47 is lower than ~0.58 of flexible chains in the intermediate solvent and is even smaller than 0.50 in the θ-state [18,31,38–40], but is comparable to the experimental value 0.44 found by Park and Choi [31] for the branched polyethyleneimine having a compact structure. Accordingly, this simple comparison of experimental results lead us to postulate that the chains of PEOz may exist in the form of a somewhat compact sphere.

3.6. Size ratios of different radii for the PEOz

The values of four different size parameters and their ratios for PEOz are summarized in Table 2, and Table 3 compares the average values of each size ratio of PEOz with those of various models. In addition, $\langle R_G^2\rangle^{1/2}$ is taken as the basis for the comparison because it is the dimension that can be directly obtained from the light scattering experiment.

All the size ratios listed in Table 2 show a trend of molar mass independence, which means that they are universal ratios [41]. The $\langle R_G^2\rangle^{1/2}/R_H$ value of 1.21 for PEOz is in reasonable accordance with the recent theoretical estimation of 1.24 predicted for the non-draining Gaussian chain by Oono and Kohomoto [27] in their renormalization group calculation. Furthermore, a comparison of this 1.24 with the experimental finding of 1.28 [42] in a θ-system (PS/cyclohexane) and 1.5–1.7 [43] of the non-draining in a good solvent makes it clear that the $\langle R_G^2\rangle^{1/2}/R_H$ of PEOz is substantially small, indicating dimensional contraction, but far from that of a hard sphere.

The R_Ts found are slightly larger than $\langle R_G^2\rangle^{1/2}$ values, but they reflect a strong molar mass dependence, as is shown in Fig. 6, which means that the excluded-volume effect vanishes as the molar mass decreases. Unexpectedly, however, the average value of 0.97 for the size ratio $\langle R_G^2\rangle^{1/2}/R_T$ is far less than the 1.79 for linear PS in 2-butanone [18] and is also found to be even smaller than the 1.42 predicted for the non-draining Gaussian chain [44], but it approaches the 0.96 for the six-arm star PS [45]. Recently, similar behavior has been observed also by Fetters et al. [40] for the system of polyisobutylene dilute solution. This is due, in part, to both the sensitivity of R_T to the solvent quality and the high sensitivity of $\langle R_G^2\rangle^{1/2}$ to the larger dimension of non-spherical objects. At any rate, this smaller $\langle R_G^2\rangle^{1/2}/R_T$ ratio is an indication of the sphere-like shape.

Those values of $\langle R_G^2\rangle^{1/2}$ and R_V listed in Table 2 exhibit almost the same order of magnitude, particularly in the higher molar mass range, and hence give an almost constant ratio of $\langle R_G^2\rangle^{1/2}/R_V$. The average value 0.996 does not agree well with the theoretical values of 1.24 in a good solvent [17] and 0.78 for a hard sphere, but is comparable with 1.09 for a four-arm star PB/toluene [46]. The lower ratio of this study probably results from the lower degree of contribution of $\langle R_G^2\rangle^{1/2}$ than R_V to the ratio because R_V is affected by both the static and dynamic contributions.

The R_V/R_H ratio shows no tendency of molar mass dependence, and the average value is found to be 1.22, which is similar to the theoretical value of 1.23 [47] for unperturbed coils, but is substantially larger than 1.0 for the hard sphere, 1.07 [17] for PS in θ, and 1.15 for some other flexible chains in thermodynamically moderate solvents [48]. Concurrently, experimental values of 0.95–1.2 [49,50] and 1.185 [41] of R_V/R_H are reported for several branching architectures and PαMS in butyl chloride, respectively. The ratio of the present work is consistent with the value of 1.2 for some branched chains and also with the experimental results stating that the ratio becomes larger when the chain is in a thermodynamically moderate solvent than in either a good solvent or a θ-solvent [41]. As exemplified above, there are wide discrepancies between R_V/R_H values for different polymer–solvent systems. To take the value 1.22 into account, although the reason for the above difference is not apparent, the chains of PEOz may take probably a somewhat distorted sphere-like shape [18].

3.7. Unperturbed molecular dimension of PEOz

Practically, searching for a θ-solvent of a new polymer is

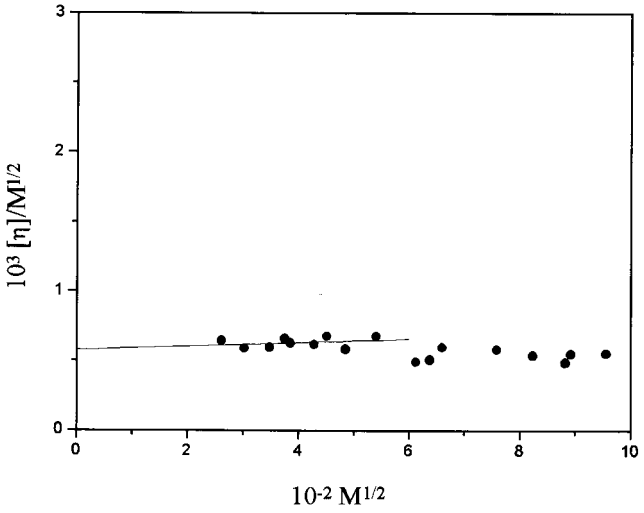

Fig. 9. Stockmayer–Fixman plot for PEOz in THF at 25°C.

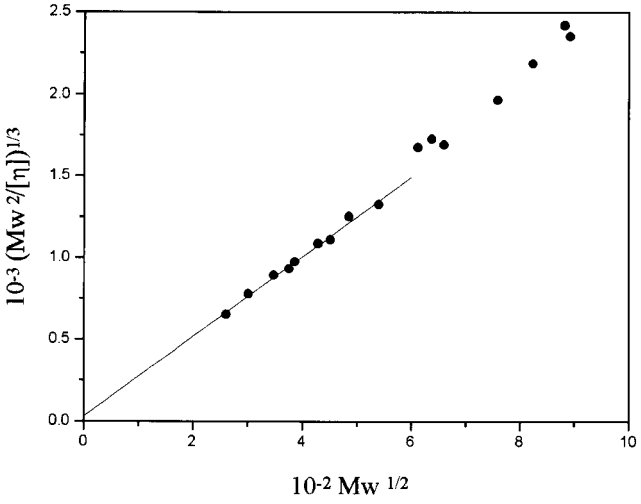

Fig. 10. Plot of $(M_w^2/[\eta])^{1/3}$ versus $M_w^{1/2}$ in THF at 25°C.

very difficult. Thus, the unperturbed chain dimensions are often estimated by employing indirect approaches [14]. The foremost of these investigations is a viscosity plot attempted by Burchad, Stockmayer, and Fixman (BSF) [51,52].

In Fig. 9 the plots of $[\eta]/M_w^{1/2}$ versus $M_w^{1/2}$, which display two parts separated by a "break" point, are illustrated. The small slope of the high molar mass range may result from the formation of a sphere-like structure from the random coil with increasing molar mass. The extrapolation, on the other hand, of the straight line drawn below the "break" point region ($M_w < 2.9 \times 10^5$ g/mol) gives the unperturbed molecular dimension of $(\langle R^2 \rangle)_0/M_w)^{1/2} = 624 \times 10^{-4}$ nm. Comparing this value with atactic PMMA (640×10^{-4} nm) and PS (670×10^{-4} nm) in various solvents [24] shows that the low molar mass chains of PEOz may exist as a random coil but become gradually a sphere-like structure with increasing molar mass.

Additionally, an estimation of the persistence length q of the PEOz chain is attempted. The approaches proposed by Bushin and Bohdanecky [16,53], respectively, can be expressed as follows:

$$(M_w^2/[\eta])^{1/3} = A_\eta + B_\eta M_w^{1/2} \tag{12}$$

with

$$A_\eta = A_0 M_L \Phi_\infty^{-1/3} \tag{13}$$

$$B_\eta = B_0(\langle R_G^2 \rangle_0/M_w)_\infty^{-1/2} \Phi_\infty^{-1/3} \tag{14}$$

where Φ_∞ is the Flory viscosity factor for an unperturbed random coil and A_0 and B_0 are given as a function of $d/2q$, where d is the diameter of the worm-like cylinder model. Fig. 10 shows the $[\eta]$ data in THF at 25°C according to Eq. (12). The data points closely follow the straight line but deviate from that upward at molar masses above 4.9×10^5 g/mol. This upswing, as noted above, is ascribed to the formation of a typical sphere-like shape of high molecular mass molecules. The intercept and slope of the initial straight line in Fig. 10, allow us to estimate $A_\eta = 23.58$ g$^{1/3}$ cm^{-1} and $B_\eta = 2.41$ g$^{1/3}$ cm^{-1}, respectively. Since $[\eta]$ is rather insensitive to d, an approximate value of $d = 0.90$ nm is estimated from the molecular model of PEOz. From the intercept A_η, the persistence length q was estimated as $q = 0.70$ nm. Although there remains a doubt regarding the accuracy of the estimated q value owing to the very low value of the intercept, the q value found is clearly far below the range that a typically flexible polymer chain can exhibit (1.2 nm). This result is ascribed tentatively to the molecular contraction that arose from the side group effect on $[\eta]$ and the intramolecular specific interaction between nitrogen and carbonyl carbon in the main chain and the side group, respectively.

According to Allegra et al. [19], on the other hand, the statistical configuration of the chains inside the collapsed globules was predicted to depend on the ratio $R = \langle R_G^2 \rangle^{1/2}/q$, under the assumption that the chemical structure is homogeneous. If R is much larger than unity, as happens in particular with long PS molecules, the chain can be regarded as a "random Gaussian globule" [33]. The R value found for the present PEOz was 24, which implies that the chain conformation is like that of a "random Gaussian globule".

4. Conclusions

The equilibrium molecular shape of well-defined PEOz in THF at 25°C is investigated by light scattering and viscometry. Those power laws established from the molar mass dependences of z-average radius of gyration $\langle R_G^2 \rangle^{1/2}$, second virial coefficient A_2, intrinsic viscosity $[\eta]$, various radii (R_H, R_T, R_V), and size ratio parameters, allow us to conclude that the overall shape of a PEOz molecule is sphere-like, being very similar to a "random Gaussian globule", in the least draining limit. The low molar mass fractions ($M_w < 2.9 \times 10^5$) are found to exist as random coils, but transform

gradually to the form of a sphere-like structure with the increment of molar mass.

The uniformity in the side group length of PEOz and the intramolecular polar interaction between the nitrogen in the backbone chain and the carbonyl carbon in the side group is considered to be responsible for the contraction of the molecular dimension. Assuming that the chains can be separated fully from each other in the medium of dilute solution, the overwhelming fractions of the chains are expected to undergo intramolecular specific interactions easily.

Acknowledgements

This work was partly supported financially by the Research Center of Inha University.

References

[1] Tomalia DA, Sheetz DP. J Polym Sci Part A-1 1966;4:2253.
[2] Bassiri TG, Levy A, Litt M. J Polym Sci Part B 1967;5:871.
[3] Gagiya T, Matsuda T. J Macromol Sci Chem 1972;A6:135.
[4] Saegusa T, Iroharu H, Fujii H. Polym J 1972;3:176.
[5] Saegusa T, Ikeda H. Macromolecules 1973;6:808.
[6] Litt M, Levy A, Herz J. J Macromol Sci Chem 1975;A9:815.
[7] Miyamoto M, Aoi K, Saegusa T. Macromolecules 1991;24:11.
[8] Kagiya T, Mastuda T. J Macromol Sci Chem 1971;A5:1265.
[9] Saegusa T, Ikeda H, Fujii H. Macromolecules 1973;5:315.
[10] Saegusa T, Kobayashi S, Yamada A. Makromol Chem 1976;177:2271.
[11] Chen FP, Ames AE, Taylor LD. Macromolecules 1990;23:46,888.
[12] Goddard P, Hutchinson LE, Brown J, Brookman J. J Controlled Release 1989;10:5.
[13] Keskkula H, Paul DR. J Appl Polym Sci 1986;31:1189.
[14] Yamakawa H. Modern theory of polymer solution. New York: Harper and Row, 1971.
[15] Yamakawa H, Yoshizaki T. Macromolecules 1980;13:633.
[16] Bohdanecky M. Macromolecules 1983;16:1483.
[17] Douglas JF, Roovers J, Freed KF. Macromolecules 1990;23:4168.
[18] Lewis ME, Nan S, Yunan W, Li J, Mays JW, Hadjichristidis N. Macromolecules 1991;24:6686.
[19] Allegra G, Ganazzoli F, Raos G. Trends Polym Sci 1996;4:293.
[20] Van Krevelen DW. Properties of polymers. 3rd ed. Amsterdam: Elsevier Science, 1990.
[21] Huglin MB. Light scattering from polymer solutions. New York: Academic Press, 1972.
[22] Brown W. Dynamic light scattering. Oxford: Clarendon Press, 1993 (chap. 4).
[23] Bagley EB, Nelson TP, Scigliniano JM. J Paint Technol 1971;43:35.
[24] Brandrup J, Immergut EH. Polymer handbook. 2nd ed. New York: Wiley, 1975.
[25] Flory PJ. J Chem Phys 1949;17:303.
[26] Douglas JF, Freed KF. Macromolecules 1985;18:201.
[27] Oono Y, Kohomoto M. J Chem Phys 1983;78:520.
[28] Flory PJ, Krigbaum WR. J Chem Phys 1950;18:1086.
[29] Fujita H. Polymer solution. Amsterdam: Elsevier, 1990 (chap. 2).
[30] Chen CH, Wilson J, Chen W, Davis RM, Riffle JS. Polymer 1994;35:3587.
[31] Park IH, Choi EJ. Polymer 1996;37:313.
[32] Weill G, Cloizeaux D. J Phys (Paris) 1979;40:99.
[33] Allegra G, Ganazzoli F. J Chem Phys 1985;83:397.
[34] Bohdanecky M, Kovar J. Viscosity of polymer solution. Amsterdam: Elsevier Science, 1982 (chap. 3).
[35] Fujii Y, Tamai Y, Konishi T, Yamakawa H. Macromolecules 1991;24:1608.
[36] Karata M, Fukatsu M. J Chem Phys 1964;41:2934.
[37] Wolfe JF, Stille JK. Macromolecules 1976;9:489.
[38] Lewis ME, Nan S, Mays JW. Macromolecules 1991;24:197.
[39] Weill G, Cloizeaux JD. J Phys (Les Ulis Fr) 1979;40:99.
[40] Fetters LJ, Hadjichristidis N, Lindner JS, Mays JW, Wilson WW. Macromolecules 1991;24:3127.
[41] Mays JW, Nan S, Lewis ME. Macromolecules 1991;24:4857.
[42] Schmidt M, Burchard W. Macromolecules 1980;13:657.
[43] Park S, Chang T, Park IH. Macromolecules 1991;24:5729.
[44] Oono Y. J Chem Phys 1983;79:4629.
[45] Roovers J, Martin JE. J Polym Sci Polym Phys Ed 1989;27:2513.
[46] Roovers J, Toporowski PM. J Polym Sci Polym Phys Ed 1980;18:1907.
[47] Pyun CW, Fixman M. J Chem Phys 1964;41:937.
[48] Lindner JS, Wilson WW, Mays JW, Hadjichritidis N, Fetters LJ. In preparation.
[49] Wang QW, Park IH, Chu B. Am Chem Soc Symp Ser 1987;352:240.
[50] Bauer BJ, Fetters LJ, Graessley WW, Hadjichristidis N, Quack GF. Macromolecules 1989;22:2337.
[51] Burchad W. Makromol Chem 1960;50:20.
[52] Stockmayer WH, Fixman M. J Polym Sci Part C 1963;1:137.
[53] Bushin SV, Tsvetkov VN, Lysenko EB, Emel'yanoov VN. Vysokomol Soedin 1981;A23:2494.
[54] Fixman M. J Chem Phys 1986;84:4085.
[55] Freed KF, Wang SQ, Roovers J, Douglas J. Macromolecules 1988;21:2219.